Ferroelectricity Driven by Y d^0-ness with Rehybridization in $YMnO_3$

D.-Y. Cho,[1] J.-Y. Kim,[2] B.-G. Park,[3] K.-J. Rho,[3] J.-H. Park,[2,3,*] H.-J. Noh,[1] B. J. Kim,[1] S.-J. Oh,[1] H.-M. Park,[4] J.-S. Ahn,[5] H. Ishibashi,[5] S-W. Cheong,[5] J. H. Lee,[6] P. Murugavel,[6] T. W. Noh,[6] A. Tanaka,[7] and T. Jo[7]

[1]*CSCMR & School of Physics and Astronomy, Seoul National University, Seoul 151-747, Korea*
[2]*Pohang Accelerator Laboratory, Pohang University of Science and Technology, Pohang 790-784, Korea*
[3]*eSSC & Department of Physics, Pohang University of Science and Technology, Pohang 790-784, Korea*
[4]*Korea Research Institute of Standards and Science, Yusong, 305-600, Korea*
[5]*Department of Physics and Astronomy, Rutgers University, Piscataway, New Jersey 08854, USA*
[6]*ReCOE & School of Physics and Astronomy, Seoul National University, Seoul 151-747, Korea*
[7]*Department of Quantum Matter, ADSM, Hiroshima University, Higashi-Hiroshima 739-8526, Japan*

(Received 8 November 2006; published 21 May 2007)

We investigated electronic structure of hexagonal multiferroic $YMnO_3$ using the polarization dependent x-ray absorption spectroscopy (XAS) at O K and Mn $L_{2,3}$ edges. The spectra exhibit strong polarization dependence at both edges, reflecting anisotropic Mn $3d$ orbital occupation. Moreover, the O K edge spectra show that Y $4d$ states are strongly hybridized with O $2p$ ones, resulting in large anomalies in Born effective charges on off-centering Y and O ions. These results manifest that the Y d^0-ness with rehybridization is the driving force for the ferroelectricity, and suggest a new approach to understand the multiferroicity in the hexagonal manganites.

DOI: 10.1103/PhysRevLett.98.217601 PACS numbers: 77.84.−s, 71.70.Ch, 75.50.Ee, 78.70.Dm

Recently, multiferroicity, in which magnetism and ferroelectricity coexist, takes much attention due to its exotic magnetoelecric phenomena [1–3], which enable us to control magnetism through an electric field or electricity through a magnetic field and may open up a new concept of potential technological applications. Especially, RMnO$_3$, which is crystallized either in hexagonal structure for R = Ho, Er, Tm, Yb, Lu, or Y, Sc with smaller ionic radius or in the orthorhombic one for R = La, Ce, Pr, Nd, Eu, Gd, Tb, Dy, or Bi with larger ionic radius [4,5], exhibits different types of multiferroicity [3,4].

Hexagonal RMnO$_3$ exhibits multiferroicity with high ferroelectric and low antiferromagnetic transition temperature ($T_E > 600$ K, $T_M \sim 90$ K). The hexagonal structure ($P6_3cm$) brings out soft mode phonons required for ferroelectricity [6], but its driving force has been puzzling. A prototype ferroelectricity was observed in the so-called "d^0-ness" systems such as $BaTiO_3$, in which $Ti^{4+}(d^0)$ ions make off-center movements in TiO_6 octahedra to lower the energy through enhanced Ti $3d$–O $2p$ hybridization (rehybridization) [7,8]. RMnO$_3$, however, contains Mn^{3+} (d^4) magnetic ions, and the ferroelectricity demands a mechanism other than the d^0-ness, such as lone pair electrons in $BiMnO_3$ or a spin frustration of magnetic order in $TbMnO_3$ [3]. However, neither the lone pair nor the spin frustration could hold for the ferroelectricity of hexagonal RMnO$_3$. The system contains bipyramid MnO_5, two on-top oxygens (O_T) and three in-plane oxygens (O_P), and its unusual electronic structure has been suspected to be responsible for the ferroelectricity [9,10].

Under the MnO_5 D_{3h} site symmetry, $3d$ orbital is split into two doublets, e_{1g} (yz/zx) and e_{2g} ($xy/x^2 - y^2$), and one singlet, a_{1g} (z^2). The Mn^{3+} d^4 ground state configuration becomes $e_{1g}^2 e_{2g}^2$, and Mn $3d$ states have strong anisotropic bonding with O $2p$ ones along the hexagonal c axis, which is the ferroelectric direction. Then "directional" Mn d^0-ness was suggested as the origin of the ferroelectricity [9]. However, actual polarization was found to be induced from off-center movements of Y-O_P sites rather than Mn-O_T sites [11]. Meanwhile, van Aken *et al.* claimed based on local density band calculations that Y-O_P off-center movements are stabilized entirely due to electrostatic energy since Y-O bonds are almost ionic and so do not contribute large anomalies in Born effective charges [12], which are directly related to the polarization, on the acting Y-O_P sites [13]. However, the predicted site movements are considerably different from the actual ones, and the estimated stabilization energy is much smaller than $T_E \sim 1000$ K. The differences could be reduced by optimizing the lattice coordinates in an LSDA + U (local spin density approximation plus Hubbard U) method [10,14], but the predicted electronic structure is far away from the experimental one.

In this Letter, we scrutinized the electronic structure and Mn-O and Y-O bond characteristics in $YMnO_3$ using the polarization dependent x-ray absorption spectroscopy (XAS) at O K edge, which reflects the unoccupied conduction band. The strict selection rules of the polarization dependent XAS enable us to confidently identify the hybridized Mn $3d$ and Y $4d$ states. The detailed spectral features were found to be away from the band calculation results but well described in terms of the cluster model calculations for MnO_5 and YO_8. The analysis for the Mn $3d$ region in the O K edge XAS, which shows strong anisotropic hybridization, describes consistently the Mn $L_{2,3}$ edge polarization dependent XAS results. Interestingly,

the Y 4d region in the O K edge XAS also reveals strong anisotropic Y 4d-O 2p hybridization, especially along the c-axis polarization direction. The strong Y 4d-O 2p hybridization contributes large anomalies in Born effective charges on the off-centering Y-O_P sites. Further, the XAS spectra at O K- and Mn $L_{2,3}$ edges of hexagonal $DyMnO_3$/Pt(111) and orthorhombic $DyMnO_3/SrTiO_3(001)$ show very similar polarization dependence to those of hexagonal $YMnO_3$ and orthorhombic $LaMnO_3$, respectively. These results manifest that in hexagonal $RMnO_3$, the R d^0-ness with rehybridization is commonly responsible for the ferroelectricity.

A high quality $YMnO_3$ single crystal was grown by using the floating zone method [15], and oriented through the Laue diffraction. As shown in the inset of Fig. 1(a), Mn^{3+} and Y^{3+} ions have MnO_5 and YO_8 local structures with bipyramidal D_{3h} and trigonal D_{3d} site symmetries, respectively. A clean $YMnO_3$ crystal was prepared to expose a hexagonal $[0001] \times [10\bar{1}0]$ plane, in which the c axis is in the plane, to the incoming light, and was introduced into an experimental chamber under 4×10^{-10} Torr. The measurements were performed at the 2A elliptically polarized undulator beam line in the Pohang light source (PLS). Taking advantage of controllability of photon polarization, we could obtain the polarization dependent XAS spectra without changing any experimental geometry. The sample temperature was kept at room temperature, and the energy resolution was set to be about 0.15 eV. The O K edge spectra were simultaneously collected in both total electron yield (TEY) and fluorescence yield (FY) modes, confirming that surface degradation effects were negligible.

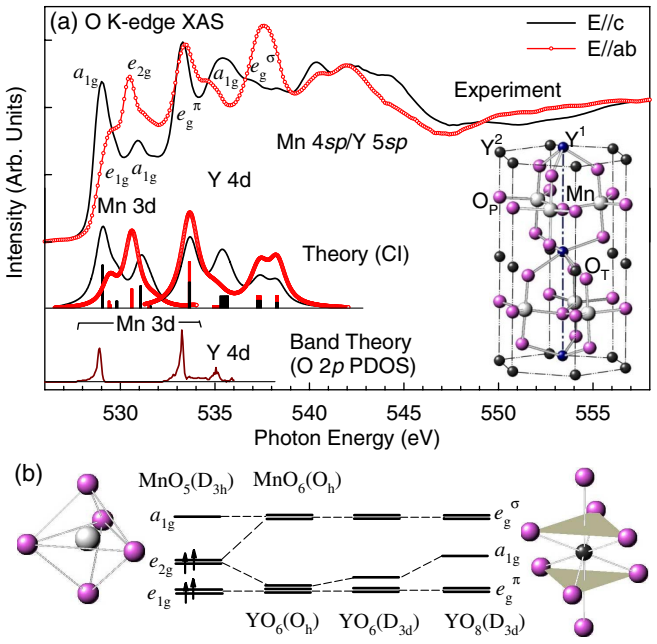

FIG. 1 (color online). (a) O K edge polarization dependent XAS spectra of hexagonal $YMnO_3$ collected in FY mode in comparison with the CI model calculations and the band calculations taken from Ref. [13] for O 2p PDOS. The crystal structure is shown in the inset. The solid bars represent the intensities of the delta functions. (b) Schematic crystal field splittings for MnO_5 (D_{3h}) and YO_8 (D_{3d}).

Figure 1(a) shows the O K edge polarization dependent XAS spectra ($E \parallel c$ and $E \parallel ab$) of $YMnO_3$. The spectra, which directly show transferred O 2p partial density of states (PDOS) due to hybridization to the unoccupied conduction bands, are roughly divided into Mn 3d, Y 4d, and Mn 4sp/Y 5sp regions. The spectrum exhibits strong polarization dependence in the Mn 3d and Y 4d regions, indicating strong Mn 3d-O 2p and Y 4d-O 2p bond anisotropy, respectively. The Mn 3d region consists of four major features, which can be identified as a_{1g} ($z^2_\uparrow$), e_{1g} ($yz_\downarrow/zx_\downarrow$), e_{2g} ($xy_\downarrow/x^2-y^2_\downarrow$), and a_{1g} ($z^2_\downarrow$) as denoted in Fig. 1(a). The more detailed features were analyzed by using the cluster model calculations including the configuration interaction (CI) and atomic full multiplets [16], as compared in the figure. In the model calculation, Mn 3d-O 2p hybridizations were presented by the Slater-Koster transfer integrals, $V_{pd\sigma}$ and $V_{pd\pi}$ with $V_{pd\sigma} = -2V_{pd\pi}$ [17]. The Harrison's rule ($d^{-3.5}$) was applied for different interatomic distances to the transfer integrals [18]. The bipyramid MnO_5 local structure leads about 3 times larger effective hybridization strength for the z^2 orbital than for other orbitals. The Mn^{3+} ($3d^4$) ionic ground state was found to be $S = 2$ with empty z^2 orbital. Considering the O 1s core-hole energy difference (0.4 eV) of O_T and O_P in the final state, we found that the energies relative to the a_{1g} ($z^2_\uparrow$) lowest energy state are 0.4 eV (e_{1g}), 1.1 eV (e_{2g}), and 1.9 eV (a_{1g}), very consistent with the previous reports [19].

The Y 4d region consists of three major features, corresponding to a doublet e^π_g, a singlet a_{1g}, and a doublet e^σ_g orbital as denoted in Fig. 1(a). Y ions are surrounded by six O_T and two O_P ions, i.e., YO_8, with a D_{3d} trigonal site symmetry. The crystal field splittings are schematically depicted in Fig. 1(b). The spectral features were also analyzed by using the cluster model calculations. The calculated spectra presented in Fig. 1(a) agree well with the experiments for both $E \parallel c$ and $E \parallel ab$. Y 4d-O 2p hybridization is so strong that it contributes even larger intensity (O 2p PDOS) than the Mn 3d-O 2p one, in contrast to the band calculations [13], which predict that Y 4d-O 2p hybridization is negligible. As also compared in the figure, the O 2p PDOS quoted from the band calculations is far away from the spectra even in the Mn 3d region, indicating that the one-electron approximation may not be appropriate for this material. Further, the spectra show that the a_{1g} state, which mainly hybridizes with O_P ions along the c axis, has quite large transferred O 2p weight. Considering the fact that the off-center movements mostly occur at Y-O_P sites, such a large amount of transferred charge must contribute large anomalies in Born effective charges on the ions.

Figure 2 shows local structures of MnO_5 and YO_8 in ferroelectric and centrosymmetric lattices [20]. The MnO_5

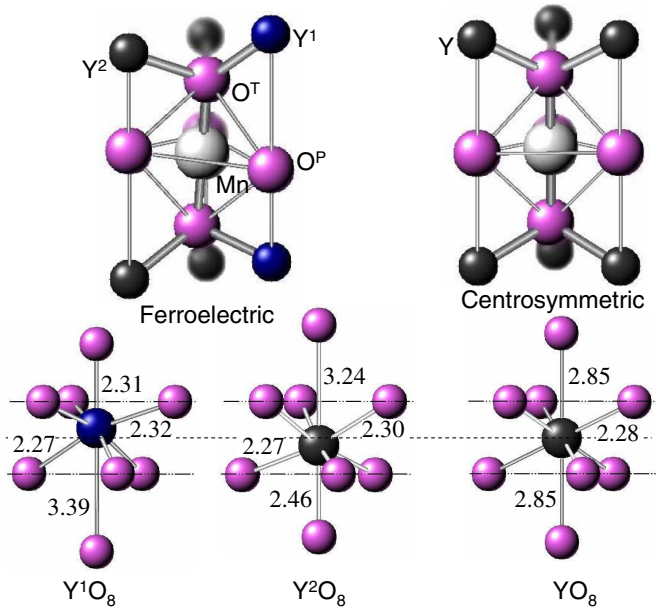

FIG. 2 (color online). Local structures of MnO_5 and YO_8 (Y^1O_8 and Y^2O_8) cages in ferroelectric and the centrosymmetric phases.

cage simply rotates with the ferroelectric distortions without off centering. The large off-center movements occur at Y^1O_8 and Y^2O_8 cages. Y-O_T bond lengths barely change but Y^1-O_P and Y^2-O_P bond lengths change by huge amounts, 23% (0.54 Å) and 17% (0.39 Å) of the ordinary Y-O distance, 2.3 Å, as in Y_2O_3, and according to the Harrison's rule for the p-d hybridization, $|V_{pd}| \propto d^{-3.5}$ [18], the O_P-Y-O_P hybridization strengths, $|V_{pd}|^2$, are enhanced by 73% and 34%, which contribute 8% and 4% enhancements to the total p-d hybridization strengths of Y^1O_8 and Y^2O_8, respectively. These enhancements are comparable to 5% enhancement in $BaTiO_3$ (TiO_6).

Using the Harrison's bond-orbital model [18], one can roughly estimate Born effective charges which are defined as sums of static charges and additional dynamic contributions. The static charge is reduced from the ionic value by the amount of transferred charges due to hybridization. The dynamic contribution originates in additional charge transfer due to a variation of the interatomic distance. For a p-d orbital hybridization, the amount of transferred charge (ΔZ) corresponds to $\sim |V_{pd}^{\mathrm{eff}}|^2/(\epsilon_d - \epsilon_p) \propto d^{-7}$, and the dynamic contribution does to $-7 \times \Delta Z$ in the first order perturbation; i.e., both are proportional to the amount of transferred O $2p$ electrons through the hybridization [8]. Here $|V_{pd}^{\mathrm{eff}}|^2$ and $\epsilon_d - \epsilon_p$ denote the effective summation of the p-d hybridizations for different orbitals and the charge transfer energy, respectively. The O K edge XAS shows that the transferred O $2p$ PDOS through Y $4d$-O $2p$ hybridization is much larger (more than ~40%) than that through Mn $3d$-O $2p$ one, and is expected to be larger than that through Ti $3d$-O $2p$ one in $BaTiO_3$ [21]. It is because the stronger Y $4d$-O $2p$ hybridization sufficiently compensates the larger charge transfer energy. Considering the large $|V_{pd}^{\mathrm{eff}}|^2/(\epsilon_d - \epsilon_p)$ and the hybridization enhancement due to the ferroelectric movements in the Y $4d$-O $2p$ bonds, the dynamic contribution in Born effective charges on Y and O_P ions should be comparable or even larger than those on Ti and $O_{\|}$ ions in $BaTiO_3$. Here we cannot exactly estimate the Born effective charges of Y and O_P [22], but one can easily expect that those are at least similar to those of Ti ($\sim +7$) and $O_{\|}$ (~ -6) in $BaTiO_3$ [8]. Hence the polarization in $YMnO_3$ is certainly dominated by the large dynamic contributions in Born effective charges, rather than the electrostatic charges, and the ferroelectric instability must be attributed to the Y d^0-ness with rehybridization, in an analogy to the Ti d^0-ness in $BaTiO_3$. Such large Born effective charges are consistent with the high T_E. The small ferroelectric polarization (5.5 μC cm^2) in comparison with that in $BaTiO_3$ (25 μC cm^2), could be attributed to the "ferrielectric" character; the opposite polarizations between Y^1O_8 and Y^2O_8 with 1:2 ratio.

To examine the cluster model analysis for Mn $3d$ states, we analyzed polarization dependent XAS spectra at Mn $L_{2,3}$ edges with about the same parameter set [23]. The experimental spectra at Mn $L_{2,3}$ edges were compared with those of the model calculation results in Fig. 3. The calculation well reproduces the detailed spectral features not only for both polarizations ($E \parallel c$ and $E \parallel ab$) but also for the difference spectrum. This result confirms that the electronic structure can be well explained by means of the cluster model analysis including CI and atomic full multiplets.

Now we try to extend our understanding. Figure 4 shows (a) Mn $L_{2,3}$- and (b) O K edge polarization dependent XAS spectra for the hexagonal $YMnO_3$ and orthorhombic $LaMnO_3$ in comparison with hexagonal and orthorhombic $DyMnO_3$ epitaxial films grown on $Pt(111)/Al_2O_3(0001)$ and $SrTiO_3(100)$ substrates, respectively [24]. For both polarizations, the XAS spectra of $YMnO_3$ and $LaMnO_3$ show very similar line shapes to those of the hexagonal and orthorhombic $DyMnO_3$, respectively. The spectra of the hexagonal manganites exhibit strong polarization depen-

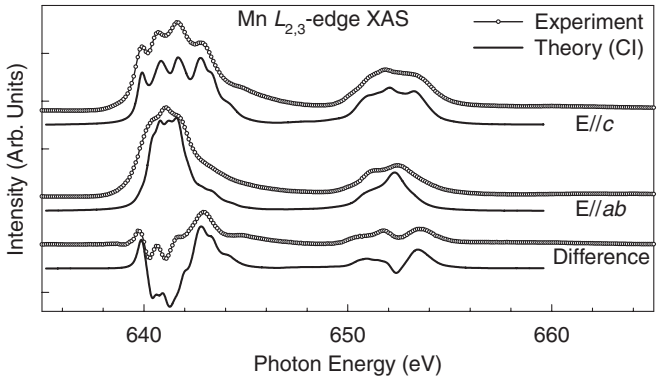

FIG. 3. Mn L edge polarization dependent XAS spectra and the difference spectrum, $(E \parallel c) - (E \parallel ab)$, of $YMnO_3$ in comparison with the CI model calculations.

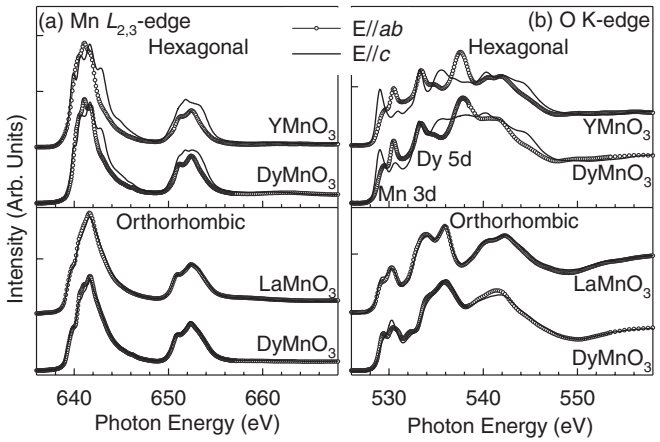

FIG. 4. Polarization dependent XAS spectra of hexagonal $RMnO_3$ (R = Y, Dy) and orthorhombic $RMnO_3$ (R = La, Dy) at (a) Mn $L_{2,3}$- and (b) O K edge collected in TEY mode. The $E \parallel c$ spectra for $DyMnO_3$ films were approximated by the spectra at $\angle(E, c) = 20°$.

dence at both Mn $L_{2,3}$- and O K edges, while the orthorhombic manganites barely show polarization dependence. It demonstrates that the ground state symmetry and the Mn $3d$-orbital energetics are mostly determined by the crystal structure. Further one can find that Dy $5d$ region in the O K edge XAS of the hexagonal $DyMnO_3$ is rather similar to the Y $4d$ region not only for the polarization dependence but also in the absorption intensity. It indicates that the hybridization strength is similar for Y $4d$-O $2p$ and Dy $5d$-O $2p$ bonds in spite of the difference of the $4d$ and $5d$ orbitals. The O K edge XAS spectrum of another hexagonal $HoMnO_3$ also shows very similar absorption intensity at the Ho $5d$ region, indicating similar hybridization in Ho $5d$-O $2p$ [25]. The identical XAS spectrum was also found at Mn $L_{2,3}$ edge for a hexagonal $ErMnO_3$ [26]. Further, the similarity in the hybridization can be also seen in other $4d$ and $5d$ oxides [27]. These results suggest that the d^0-ness scenario can be extended to other hexagonal manganites with rare-earth $5d^0$-ness.

In conclusion, we investigated the details of electronic and bond anisotropies of hexagonal $YMnO_3$. The studies show strong anisotropic hybridization not only for Mn $3d$-O $2p$ but also for Y $4d$-O $2p$ bonds. As the results, the off-center movements contribute large anomalies in Born effective charges through rehybridization. These results manifest that the ferroelectric instability is originated from the Y d^0-ness with rehybridization together with the structural phonon instability. Further we also found that the d^0-ness scenario is applicable for the ferroelectricity of other hexagonal manganites.

This work is supported by the KOSEF through the CSCMR at SNU and eSSC at POSTECH, Korean Ministry of Science and Technology through Creative Research Program at SNU, the National Science Foundation- MRSEC, POSTECH research fund, and BK21 program. Experiments at PLS were supported in part by MOST and POSTECH.

*Author to whom all correspondence should be addressed. Electronic address: jhp@postech.ac.kr

[1] N. Hur, S. Park, P. A. Sharma, J. S. Ahn, S. Guha, and S-W. Cheong, Nature (London) **429**, 392 (2004).
[2] J. Wang *et al.*, Science **299**, 1719 (2003).
[3] T. Kimura, T. Goto, H. Shintani, K. Ishizaka, T. Arima, and Y. Tokura, Nature (London) **426**, 55 (2003).
[4] H. L. Yakel, W. C. Koehler, E. F. Bertaut, and F. Forrat, Acta Crystallogr. **16**, 957 (1963).
[5] F. Moussa, M. Hennion, J. Rodriguez-Carvajal, H. Moudden, L. Pinsard, and A. Revcolevschi, Phys. Rev. B **54**, 15 149 (1996).
[6] M. N. Iliev *et al.*, Phys. Rev. B **56**, 2488 (1997).
[7] R. E. Cohen, Nature (London) **358**, 136 (1992).
[8] Ph. Ghosez, J.-P. Michenaud, and X. Gonze, Phys. Rev. B **58**, 6224 (1998).
[9] A. Filippetti and N. A. Hill, Phys. Rev. B **65**, 195120 (2002).
[10] M. Qian, J. Dong, and D. Y. Xing, Phys. Lett. A **270**, 96 (2000).
[11] T. Katsufuji *et al.*, Phys. Rev. B **66**, 134434 (2002).
[12] M. Born and M. Goppert-Mayer, Handb. Phys. **24**, 623 (1933); M. Born and K. Huang, *Dynamical Theory of Crystal Lattices* (University Press, Oxford, 1968).
[13] B. B. van Aken, T. T. M. Palstra, A. Filippetti, and N. A. Spaldin, Nat. Mater. **3**, 164 (2004).
[14] C. J. Fennie and K. M. Rabe, Phys. Rev. B **72**, 100103(R) (2005).
[15] P. A. Sharma *et al.* Phys. Rev. Lett. **93**, 177202 (2004).
[16] A. Tanaka and T. Jo, J. Phys. Soc. Jpn. **63**, 2788 (1994).
[17] The calculations were performed for $d^n \bigoplus d^{n+1}\underline{L} \bigoplus d^{n+2}\underline{L}^2$. The fitting parameters are $U_{dd} =$ 4.5 eV, $V_{pd\sigma}(z^2) = 3.8$ eV, $\Delta = 4.0$ eV, and Slater integrals were taken to be ~50% of the atomic Hartree-Fock values. Bare crystal field splitting energies were 0.5 eV for e_{1g} and e_{2g} and 0.6 eV for e_{2g} and a_{1g}. The details will be published elsewhere.
[18] W. A. Harrison, *Electronic Structure and the Properties of Solids* (Freeman, San Fransisco, 1980).
[19] M. Fiebig, Th. Lottermoser, D. Fröhlich, A. V. Goltsev, and R. V. Pisarev, Nature (London) **419**, 818 (2002).
[20] S. Lee *et al.*, Phys. Rev. B **71**, 180413(R) (2005).
[21] The transferred charge in $BaTiO_3$ was estimated to be comparable to that in $CaMnO_3$ [9].
[22] In the first order perturbation, the Born effective charges of Y and O_P are estimated to be $\sim +8$ and ~ -5, respectively.
[23] The Slater integrals and crystal field splitting energy for e_{2g} and a_{1g} were taken to be 10% larger and 25% smaller than of O K edge's to account for the core-hole effects, respectively. The $2p$-$3d$ Coulomb energy was taken to be $U_{pd} = 5.5$ eV. The uncertainty of the parameter values is estimated to be less than 10%.
[24] J. H. Lee *et al.*, Adv. Mater. **18**, 3125 (2006).
[25] K. Asokan *et al.*, Solid State Commun. **134**, 821 (2005).
[26] J.-S. Kang *et al.*, Phys. Rev. B **71**, 092405 (2005).
[27] S. J. Moon *et al.*, Phys. Rev. B **74**, 113104 (2006).